Chemistry & Biology
Article

Structural Determinants of Inhibitor Selectivity in Prokaryotic IMP Dehydrogenases

Deviprasad R. Gollapalli,[1] Iain S. MacPherson,[1] George Liechti,[2] Suresh Kumar Gorla,[1] Joanna B. Goldberg,[2] and Lizbeth Hedstrom[1,3,*]
[1]Department of Biology, Brandeis University, 415 South Street, Waltham, MA 02454-9110, USA
[2]Department of Microbiology, University of Virginia Health System, Charlottesville, VA 22908-0734, USA
[3]Department of Chemistry, Brandeis University, 415 South Street, Waltham, MA 02454-9110, USA
*Correspondence: hedstrom@brandeis.edu
DOI 10.1016/j.chembiol.2010.07.014

SUMMARY

The protozoan parasite *Cryptosporidium parvum* is a major cause of gastrointestinal disease; no effective drug therapy exists to treat this infection. Curiously, *C. parvum* IMPDH (*Cp*IMPDH) is most closely related to prokaryotic IMPDHs, suggesting that the parasite obtained its *IMPDH* gene via horizontal transfer. We previously identified inhibitors of *Cp*IMPDH that do not inhibit human IMPDHs. Here, we show that these compounds also inhibit IMPDHs from *Helicobacter pylori*, *Borrelia burgdorferi*, and *Streptococcus pyogenes*, but not from *Escherichia coli*. Residues Ala165 and Tyr358 comprise a structural motif that defines susceptible enzymes. Importantly, a second-generation *Cp*IMPDH inhibitor has bacteriocidal activity on *H. pylori* but not *E. coli*. We propose that *Cp*IMPDH-targeted inhibitors can be developed into a new class of antibiotics that will spare some commensal bacteria.

INTRODUCTION

Microbial infections are now the second leading cause of death worldwide. Many commonly used antibiotics have been rendered ineffective by the upsurge of drug resistance, and years of neglect have left a mere trickle of new antibiotics in the pipeline, creating an urgent need for novel scaffolds and targets (Fischbach and Walsh, 2009). The repurposing of other drug development programs for antibiotic discovery is a promising strategy to address this problem (Miller et al., 2009; Walsh and Fischbach, 2009). Inosine 5′-monophosphate dehydrogenase (IMPDH) presents an intriguing opportunity for such repurposing. This enzyme catalyzes the pivotal step in guanine nucleotide biosynthesis, the conversion of IMP to XMP with the concomitant reduction of NAD^+ in a reaction that involves a covalent intermediate E-XMP* (Figure 1A). The guanine nucleotide pool controls proliferation, so IMPDH inhibitors such as mycophenolic acid, merimepodib, mizoribine, tiazofurin, and ribavirin are used in immunosuppressive, cancer, and antiviral therapy. As yet, IMPDH inhibitors have not been exploited in antimicrobial applications, in part because no bacterial-selective IMPDH inhibitors have been identified (Hedstrom, 2009).

The development of IMPDH-based therapy is further complicated by the conformational gymnastics of the catalytic cycle (Hedstrom, 2009). IMPDHs have two conformational states, an open conformation that allows NAD to bind, and a closed conformation where a mobile flap binds in the NAD site (Figure 1B) (Hedstrom, 2009). The closed conformation is required for the hydrolysis of the covalent intermediate E-XMP*. Thus, the flap competes with inhibitors that bind in the NAD site, and this competition is an important determinant of inhibitor potency (Hedstrom, 2009). For example, *Tritrichomonas foetus* IMPDH is 400-fold more resistant to mycophenolic acid than human IMPDH2; ~10-fold of this difference is due to changes in the structure of the inhibitor binding site while ~40-fold can be attributed to a preference for the closed conformation (Digits and Hedstrom, 2000). Therefore, for *Tf*IMPDH, the conformational equilibrium is a more important determinant of inhibitor susceptibility than the residues that contact the inhibitor. This example illustrates the difficulty in predicting inhibitor action from IMPDH sequence.

The protozoan parasite *Cryptosporidium parvum* is a major cause of diarrhea and malnutrition and a potential bioterrorism agent (Fayer, 2004). The parasite has a streamlined purine salvage pathway that depends on IMPDH for the production of guanine nucleotides (Abrahamsen et al., 2004; Striepen et al., 2004). Surprisingly, *Cp*IMPDH is closely related to prokaryotic IMPDHs (e.g., *Helicobacter pylori* IMPDH) (Figure 1C), suggesting that its *IMPDH* gene was obtained by horizontal transfer (Striepen et al., 2002, 2004). Prokaryotic and eukaryotic IMPDHs differ in both structural features and kinetic properties (Zhang et al., 1999a), which suggests that selective inhibition should be possible. We have recently identified eight selective inhibitors of *Cp*IMPDH in a high-throughput screen targeting the NAD site (compounds **A**–**H**) (Table 1) (MacPherson et al., 2010; Maurya et al., 2009; Umejiego et al., 2008). Several of these inhibitors display antiparasitic activity in a tissue culture model of *C. parvum* infection (Umejiego et al., 2008). A program of medicinal chemistry optimization has yielded inhibitors with nanomolar affinity in several structurally distinct frameworks (MacPherson et al., 2010; Maurya et al., 2009).

Mycophenolic acid and merimepodib bind in the nicotinamide subsite of the NAD site of human IMPDH, stacking against the purine ring of E-XMP* and within a single subunit of the tetramer (Sintchak et al., 1996; Sintchak and Nimmesgern, 2000). In contrast, the X-ray crystal structure of inhibitor **C64** revealed that this inhibitor interacts with the purine ring of IMP and then

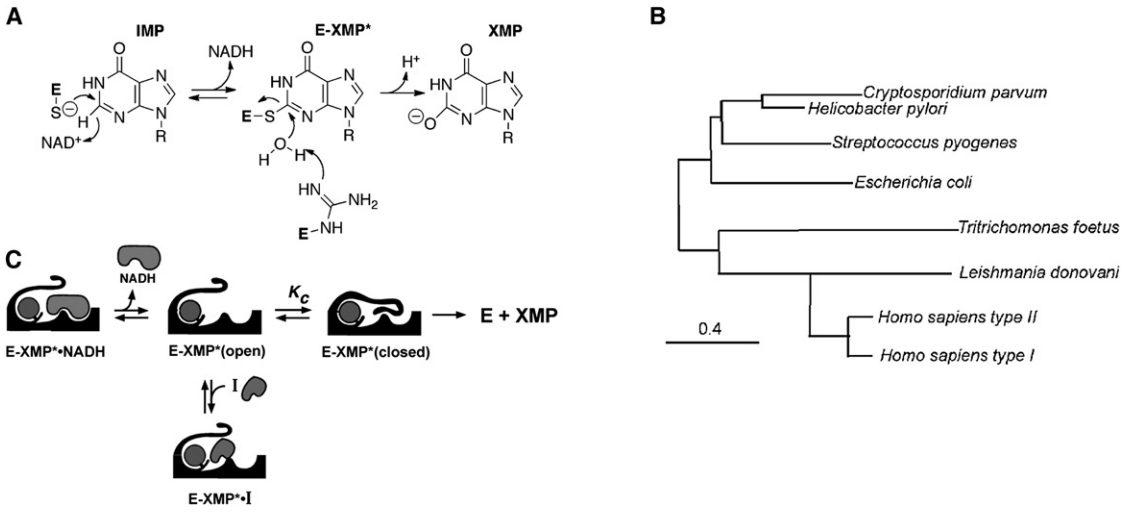

Figure 1. The IMPDH Reaction

(A) Chemical mechanism: a conserved Cys attacks C2 of IMP and hydride is transferred to NAD^+ producing the covalent intermediate E-XMP*. E-XMP* is hydrolyzed with a conserved Arg residue acting as a general base to produce XMP.

(B) Phylogenetic tree of IMPDHs.

Constructed as described in Min et al. (2008).

(C) The hydride transfer reaction proceeds in an open enzyme conformation. After NADH departs, a mobile flap folds into the NAD site, carrying the catalytic Arg into the active site. Inhibitors compete with the flap, so the equilibrium between open and closed states is a determinant of inhibitor affinity.

crosses the dimer interface to interact with Tyr358 in the adjacent subunit (Figures 2A and 2B) (*Cp*IMPDH numbering) (MacPherson et al., 2010). At present, no structures are available of the other inhibitor complexes. However, with the exception of compound **E**, all of the inhibitors contain two aromatic groups linked by spacers of similar length (Table 1) and therefore may be able to recapitulate this binding mode.

Here, we demonstrate that Tyr358 together with Ala165 comprise a structural motif that defines susceptibility to all eight *Cp*IMPDH inhibitors. This motif is found in a wide variety of pathogenic bacteria. Importantly, the *Cp*IMPDH inhibitor **C91** blocks *H. pylori* growth, but not the growth of *Escherichia coli*. These observations suggest that *Cp*IMPDH-targeted inhibitors can be developed into a new class of broader spectrum antibiotics that will spare commensal bacteria.

RESULTS AND DISCUSSION

Expression, Purification, and Characterization of Recombinant IMPDHs

We expressed and purified prokaryotic IMPDHs from representative organisms: *H. pylori* (Gram-negative ε proteobacteria), *E. coli* (Gram-negative γ proteobacteria), *B. burgdorferi* (spirochete), *S. pyogenes* (Gram-positive), and the protozoan parasite *T. foetus*, which also appears to have obtained its *IMPDH* gene from a prokaryote (Bapteste and Philippe, 2002). We also expressed an additional eukaryotic IMPDH from the protozoan parasite *Leishmania donovani*. *Ec*IMPDH, *Bb*IMPDH, *Tf*IMPDH, *Sp*IMPDH, and *Ld*IMPDH have been characterized previously (Digits and Hedstrom, 1999; Dobie et al., 2007; Kerr and Hedstrom, 1997; Zhang et al., 1999b; Zhou et al., 1997). The kinetic parameters of *Hp*IMPDH are very similar to those of *Cp*IMPDH, and are generally characteristic of bacterial IMPDHs (see Table S2 available online) (Hedstrom, 2009; Umejiego et al., 2004; Zhang et al., 1999a). Importantly, structures are available for *Tf*IMPDH, *Sp*IMPDH, and *Bb*IMPDH as well as for *Cp*IMPDH and the human enzymes (Colby et al., 1999; Gan et al., 2002, 2003; MacPherson et al., 2010; McMillan et al., 2000; Prosise and Luecke, 2003; Prosise et al., 2002; Sintchak et al., 1996; Whitby et al., 1997; Zhang et al., 1999b). *Cp*IMPDH is most closely related to *Hp*IMPDH with 60% sequence identity (Figure 1C; Table S1). The sequence of *Cp*IMPDH is ~50% identical to *Ec*IMPDH, *Bb*IMPDH, and *Sp*IMPDH and ~30% identical to *Tf*IMPDH and the eukaryotic enzymes (Table S1) (Min et al., 2008; Striepen et al., 2002). Importantly, *Hp*IMPDH, *Bb*IMPDH, and *Sp*IMPDH contain Tyr358 and are therefore expected to be susceptible to the **C** series inhibitors and perhaps also to the other *Cp*IMPDH inhibitors.

Spectrum of Inhibition of C Series Inhibitors

Compound **C** inhibits *Hp*IMPDH and *Bb*IMPDH with similar values of IC_{50} to *Cp*IMPDH (Table 1). **C** is a noncompetitive (mixed) inhibitor of *Hp*IMPDH with respect to NAD^+ (data not shown), as observed with *Cp*IMPDH (Umejiego et al., 2008). Importantly, the values of K_i and IC_{50} are similar, as expected for noncompetitive inhibition. **C** also inhibits *Sp*IMPDH, although in this case the value of IC_{50} is increased by a factor of ~60 relative to *Cp*IMPDH. No inhibition is observed at 100 μM **C** for *Tf*IMPDH, *Ec*IMPDH, and *Ld*IMPDH, as expected since these enzymes do not contain Tyr358.

We also evaluated the spectrum of a second-generation inhibitor, **C91**, arising from our medicinal chemistry optimization program (S. Kirubakaran, S.K.G., C.R. Johnson, M. Zhang, D.R.G., L.H., and G.D. Cuny, unpublished data); this compound is a potent inhibitor of *Cp*IMPDH with IC_{50} = 8 nM. **C91** is also a potent inhibitor of both *Hp*IMPDH and *Sp*IMPDH,

Table 1. Inhibition of IMPDHs by Compounds A–H

Compound	IC_{50} (μM) *Cp*IMPDH[a]	*Hp*IMPDH	*Bb*IMPDH	*Sp*IMPDH	*Ec*IMPDH- S250A/L444Y
A 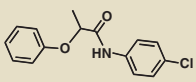	3.3 *0.66*	2.2 *1.1*	1.4 *0.84*	96 *12*	1.8 *0.54*
B 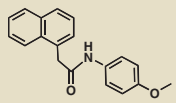	1.6 *0.32*	1.3 *0.65*	1.8 *1.1*	85 *11*	0.70 *0.21*
C 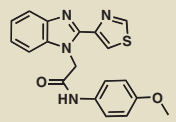	1.2 *0.24*	0.60 *0.30*	0.60 *0.36*	70 *9.1*	0.60 *0.18*
D 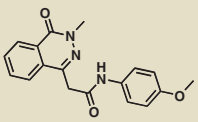	5.4 *1.1*	3.0 *1.5*	1.7 *1.0*	49 *6.4*	2.3 *0.69*
E 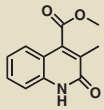	1.6 *0.32*	1.5 *0.75*	0.90 *0.54*	15 *2.0*	1.8 *0.54*
F 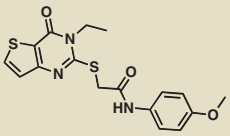	1.4 *0.28*	1.1 *0.55*	0.80 *0.48*	13 *1.7*	1.1 *0.33*
G 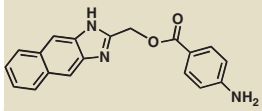	0.1 *0.02*	0.30 *0.15*	0.22 *0.13*	0.55 *0.07*	0.40 *0.12*
H 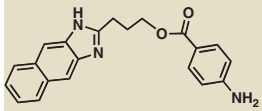	0.9 *0.18*	1.2 *0.6*	0.90 *0.54*	0.86 *0.11*	1.0 *0.3*
C91 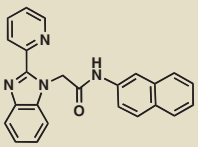	0.008[b,c] *0.0016*	0.0011[b,d] *0.0005*	n.d.	0.0054[b,c] *0.0007*	0.0019[b,e] *0.0006*

These compounds (100 μM) do not inhibit *Ec*IMPDH, *Tf*IMPDH, and *Ld*IMPDH. The errors on the IC_{50} values were less than 10% unless otherwise noted. "Intrinsic" values (adjusted for the fraction of enzyme in the open conformation) are shown in italics. Supported by Figure S1.

[a] Data from Umejiego et al. (2008).

[b] Determined with a tight-binding equation.

[c] Error ≤37%.

[d] Error = 73%;

[e] Error = 52%.

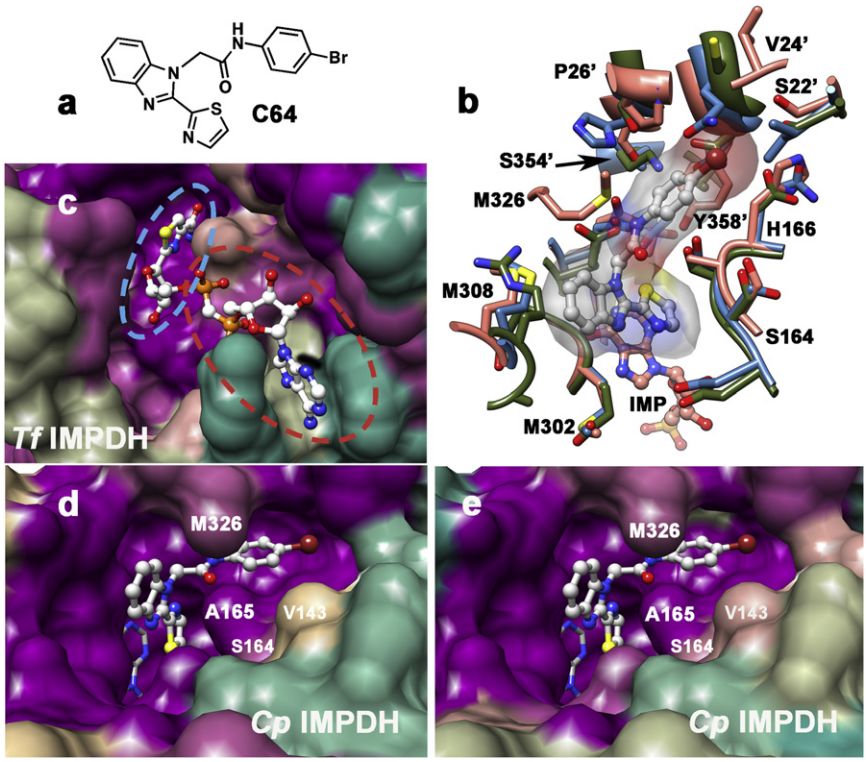

Figure 2. Structures of IMPDH Inhibitor Binding Sites

(A) Structure of **C64**.

(B) Structure of the CpIMPDH•IMP•**C64** complex (salmon; PDB accession 3KHJ) (MacPherson et al., 2010) and resistant IMPDHs from *T. foetus* (green; 1LRT) (Gan et al., 2002) and Chinese hamster (blue; 1JR1, nearly identical to human IMPDH2) (Sintchak et al., 1996). Residues within 5 Å of **C64** are displayed. **C64** is shown in gray with a transparent surface; CpIMPDH residues are labeled; residue from the adjacent monomer are denoted with an apostrophe. Residues Thr221 and Glu329 are hidden under **C64**.

(C) The surface of the NAD binding site rendered by conservation of residues in prokaryotic IMPDHs from *T. foetus*, *C. parvum*, *H. pylori*, *B. burgdorferi*, *S. pyogenes*, and *E. coli*. Dark magenta, 100% conserved; tan, 63%; dark cyan, 25%. The NAD analog tiazofurin adenine dinucleotide (TAD) is light gray. The tiazofurin binding site is circled in blue and the ADP binding site is circled in red.

(D) The surface of the **C64** binding site rendered by conservation of residues in sensitive IMPDHs from *C. parvum*, *H. pylori*, and *B. burgdorferi*, as well as the S250A/L444Y variant of *Ec*IMPDH. Ser164, Met326, and Ser354 are within 5 Å of **C64**; Val143 is 8 Å away. Dark magenta, 100% conserved; tan, 60%; dark cyan, 20%. **C64** depicted in ball-and-stick in light gray and IMP is shown in stick in dark gray.

(E) The surface of the **C64** binding site rendered by conservation of residues in *Cp*IMPDH and IMPDHs from 19 pathogenic bacteria: *Acinetobacter baumannii* (wound infection), *Bacillus anthracis* (anthrax), *Bacteroides fragilis* (peritoneal infections), *Brucella abortus/melitensis/suis* (brucellosis), *B. burgdorferi* (Lyme disease), *Burkholderia cenocepacia* (infection in cystic fibrosis), *Bu. mallei* (glanders), *Bu. pseudomallei* (melioidosis), *Campylobacter jejuni* (food poisoning), *C. lari* (food poisoning), *Coxiella burnetii* (Q fever), *Francisella tularensis* (tularemia), *H. pylori* (gastric ulcer/stomach cancer), *Listeria monocytogenes* (listeriosis), *Staphylococcus aureus* (major cause of nosocomial infection), *S. pyogenes* (major cause of nosocomial infections), and *S. pneumoniae* (pneumonia). Dark magenta, 100% conserved; tan, 63%; dark cyan, 25%. Alignments were constructed with CLUSTALW2 and molecular graphics images were produced using the UCSF Chimera package from the Resource for Biocomputing, Visualization, and Informatics at the University of California, San Francisco (supported by NIH P41 RR-01081) (Pettersen et al., 2004).

Supported by Figure S3.

demonstrating that potent broader spectrum inhibitors can be obtained (Table 1). **C91** fails to inhibit *Ec*IMPDH, *Tf*IMPDH, *Ld*IMPDH or human IMPDHs (IC_{50} > 10 μM).

The Conformational Contribution to Inhibitor Selectivity

As noted in the introduction, IMPDH undergoes a conformational change in the middle of its catalytic cycle that brings a mobile flap into the NAD site (Figure 1B). The competition of the flap for this site can be an important determinant of inhibitor susceptibility and might explain the low susceptibility of *Sp*IMPDH to **C** despite the presence of Tyr358 (Table 2; Guillén Schlippe and Hedstrom, 2005a, 2005b; Guillén Schlippe et al., 2004; Hedstrom, 2009; Kohler et al., 2005; Riera et al., 2008; Umejiego et al., 2004). Therefore, we determined the equilibrium between open and closed conformations (K_c) for the various IMPDHs (Table 2) Figure S3 and Supplemental Experimental Procedures for description) (Hedstrom, 2009). The values of K_c vary considerably among the prokaryotic IMPDHs, from 0.7 for *Bb*IMPDH to 140 for *Tf*IMPDH.

Tiazofurin inhibition illustrates the validity of this approach and the magnitude of the conformational contribution to inhibitor selectivity. The tiazofurin binding site is conserved among prokaryotic IMPDHs (Figure 2C), which predicts that *Cp*IMPDH, *Hp*IMPDH, *Bb*IMPDH, *Sp*IMPDH, *Ec*IMPDH, and *Tf*IMPDH should all bind tiazofurin with similar affinity, yet the measured values of K_i vary from 1 to 69 mM. When the measured values of K_i are adjusted for competition from the mobile flap, that is, by dividing by a factor of 1 + K_c to normalize for the fraction of protein in the open conformation, the resulting "intrinsic" values are indeed nearly identical, ranging from 0.3 to 0.7 mM (Table 2). In contrast, the intrinsic values of K_i for ADP range from 0.2 to 9 mM, reflecting the structural divergence of the ADP binding sites among the six enzymes (Figure 2C). Therefore, the intrinsic values reflect the structural similarity of the inhibitor binding sites.

The intrinsic values of IC_{50} for **C** are similar for *Cp*IMPDH, *Hp*IMPDH, and *Bb*IMPDH, indicating that the structures of inhibitor binding sites are also similar in these three enzymes. However, the intrinsic value of IC_{50} for **C** with *Sp*IMPDH remains 40-fold greater than *Cp*IMPDH. Figure 2 displays the conservation of the **C64** binding site among these IMPDHs. While most of the residues within 5 Å of **C64** are conserved among these enzymes, Ser164 and Met326 are variable; these residues are Thr and Leu, respectively, in *Sp*IMPDH. Perhaps these

Table 2. The Conformational Contribution to Potency of IMPDH Inhibitors

Enzyme	$K_{i\ Tzf}$ (mM)	$K_{i\ ADP}$ (mM)	K_c	$K_{int\ Tzf}$ (mM)	$K_{int\ ADP}$ (mM)
***Cp*IMPDH**[a]	1.5 ± 0.1	42 ± 6	4	0.3	8
***Hp*IMPDH**	1.3 ± 0.1	6.0 ± 0.5	1	0.7	3
***Bb*IMPDH**	1.1 ± 0.2	7.4 ± 0.6	0.7	0.7	4
***Sp*IMPDH**	8 ± 1	13 ± 2	7	0.7	2
***Tf*IMPDH**[a]	69 ± 9	31 ± 2	140	0.5	0.2
***Ec*IMPDH**	5.3 ± 0.6	10 ± 2	9	0.5	1
***Ec*IMPDH-S250A**	2.5 ± 0.3	0.10 ± 0.01	1.5	1	0.04
***Ec*IMPDH-S250A/L444Y**	1.1 ± 0.2	4.1 ± 0.7	2.3	0.3	1
***h*IMPDH2**[a]	1.3 ± 0.1	9 ± 2	≤0.2	1.3	9
***Ld*IMPDH**	8.3 ± 0.7	15 ± 2	2.3	2.5	5

As shown in Figure 1B, inhibitors compete with the mobile flap for the vacant NADH site. Therefore the observed affinity will be determined by the intrinsic affinity of the inhibitor for the NAD site and the affinity of the flap, i.e., $K_{int} = K_i/(1 + K_c)$, where K_{int} is the intrinsic affinity, K_i is the measured inhibition constant and K_c is the conformational equilibrium determined as described in Experimental Procedures. Supported by Figure S2.

[a] Data from Riera et al. (2008).

substitutions account for the lower potency of **C** with *Sp*IMPDH. In contrast, the intrinsic values of IC_{50} for **C91** are similar for *Cp*IMPDH, *Hp*IMPDH, and *Sp*IMPDH, indicating that the interactions that increase the potency of **C91** in *Cp*IMPDH are also found in the other enzymes.

Structural Determinants of C Susceptibility

To determine if the presence of Tyr358 is sufficient to install sensitivity to inhibitor **C**, we replaced the corresponding residue in *Ec*IMPDH with Tyr. The resulting variant, L444Y, has similar kinetic properties to *Ec*IMPDH, except that the value of K_m for NAD^+ is increased by 5-fold (Table S2). Unlike *Ec*IMPDH, **C** inhibits L444Y (Figure S2); however, L444Y is still ~100-fold less sensitive than *Cp*IMPDH.

Inspection of the residues within 5 Å of **C64** revealed another potential structural determinant of **C** susceptibility: Ala165 (Figure 2A). The installation of Ala at the corresponding position of *Ec*IMPDH also increased the sensitivity to **C**, although again the resulting variant, S250A, is ~100-fold less sensitive than *Cp*IMPDH (Figure S2). However, the combination of these mutations created a variant S250A/L444Y with similar sensitivity to **C** as *Cp*IMPDH (Table 1). The S250A/L444Y variant also displays similar sensitivity to **C91** (Table 1). Therefore, Ala250 and Tyr358 comprise a minimal structural motif that defines sensitivity to **C**.

All of the CpIMPDH Inhibitors Interact with Ala165 and Tyr358

The spectra of inhibition of compounds **A, B,** and **D–H** are also very similar to **C.** These seven compounds inhibit *Hp*IMPDH, *Bb*IMPDH, and *Sp*IMPDH, but not *Ec*IMPDH, *Tf*IMPDH, or *Ld*IMPDH (Table 1). These compounds are noncompetitive (mixed) inhibitors of *Hp*IMPDH with respect to NAD^+ (data not shown), as observed with *Cp*IMPDH (Umejiego et al., 2008). Most importantly, the *Ec*IMPDH variant S250A/L444Y is inhibited by **A**, **B**, and **D–H**, indicating that together Ala165 and Tyr358 define the structural motif required for susceptibility to all the *Cp*IMPDH inhibitors. Note that compound **E** has a single aromatic group and therefore must interact exclusively with Tyr358 and not with the purine ring of IMP.

Two Inhibitor Binding Modes Exist

Although the above observations indicate that all of the compounds interact with Ala165 and Tyr358, inspection of the intrinsic values of IC_{50} for all of the *Cp*IMPDH inhibitors reveals two distinct binding modes. The intrinsic values of IC_{50} of **C** range between 0.18 and 0.36 μM for *Cp*IMPDH, *Hp*IMPDH, *Bb*IMPDH, and S250A/L444Y (Table 2), reflecting the conservation of this binding site (Figure 2D) (MacPherson et al., 2010). Likewise, the intrinsic affinities of compounds **A**, **B**, **D**, **E**, and **F** are within a factor of 2 for all four enzymes, indicating that the binding sites of these compounds are also conserved. In contrast, the intrinsic values of **A–F** for *Sp*IMPDH are very different from *Cp*IMDPH, indicating that this binding site is significantly different in *Sp*IMPDH (Table 1). Only one substitution is present within 3.5 Å of **C64**: Met326 is a Leu in *Sp*IMPDH. However, the Leu substitution is also present in *Hp*IMPDH and *Bb*IMPDH and therefore cannot account for the different susceptibility. The next nearest substitution is Thr for Ser164; the side chain of Ser164 is 5 Å away from **C64**, but might be closer to **A**, **B**, and **D–F**.

A different trend is observed in the intrinsic affinities of **G** and **H**. *Sp*IMPDH is most similar to *Cp*IMPDH, while *Hp*IMPDH and *Bb*IMPDH display lower affinities for these compounds (Table 2). These observations suggest that **G**/**H** bind in a region that is conserved in *Sp*IMPDH and *Cp*IMPDH, but different in the other enzymes. Therefore, at least a portion of the **G**/**H** binding site must be distinct from the site that binds **A–F**. Figure S3 reveals regions of conservation between *Cp*IMPDH and *Sp*IMPDH that are not shared with the other sensitive enzymes. These regions could serve as the binding site for **G**/**H**.

Inhibition of *H. pylori* Growth

We chose to investigate the antibiotic potential of IMPDH inhibition in *H. pylori* because *Hp*IMPDH is most similar to *Cp*IMPDH. *H. pylori* causes gastrointestinal ulcers and stomach cancer; standard treatment involves triple therapy of a proton pump inhibitor, clarithromycin, and amoxicillin or metronidazole (Selgrad and Malfertheiner, 2008). Moreover, resistance is developing to the standard triple therapy, and few new antibiotics are in the pipeline. *H. pylori* has complex growth requirements that necessitate the use of rich media containing xanthine and guanine (Brucella broth) (Tomb et al., 1997). *H. pylori* will be resistant to IMPDH inhibitors if its salvage pathways can provide sufficient guanine nucleotides to support proliferation. Therefore, this bacteria provides a demanding test for the antibiotic potential of IMPDH-targeted inhibitors.

Figure 3 shows that 20 μM **C91** is sufficient to block the proliferation of a *H. pylori* culture exiting stationary phase. Higher concentrations of **C91** display bactericidal effects, with only 23% of the colony forming units remaining after 24 hr treatment with 200 μM. Exponentially growing *H. pylori* cells are also

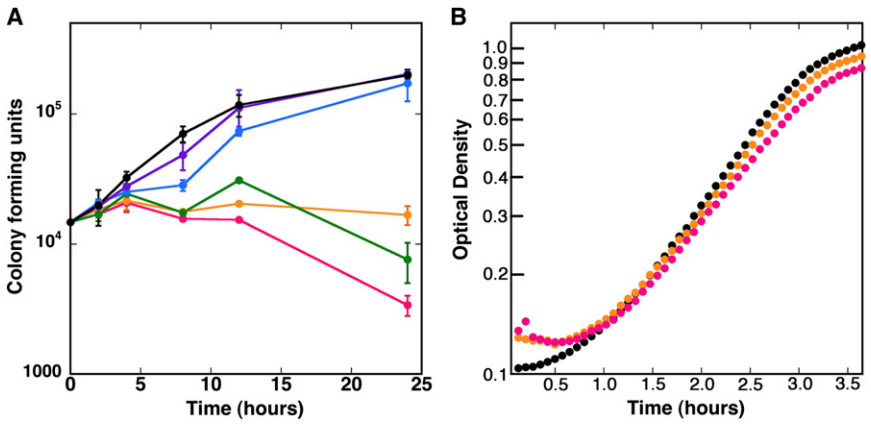

Figure 3. C91 Inhibits *H. pylori* Growth

(A) Compound **C91** in DMSO was added to freshly diluted stationary cultures of *H. pylori* strain G27 in Brucella broth. Samples were removed at the indicated time points, diluted, and plated to determine bacterial proliferation/survival. Each point is the average of duplicate determinations; a representative of three experiments is shown. Black, DMSO alone. **C91** concentrations: purple, 2 μM; blue, 7 μM; green, 20 μM; orange, 60 μM; red, 200 μM.

(B) Compound **C91** was added to freshly diluted cultures of *E. coli* MG1655 in Luria broth. Each point is the average of three determinations; the standard deviations are smaller than the point. Black, DMSO alone. **C91** concentrations: orange, 100 μM; red, 200 μM.

Supported by Figure S4.

sensitive to **C91** (Figure S1); a concentration of 60 μM is sufficient to block growth while higher concentrations are bactericidal. Importantly, **C91** failed to inhibit the growth of *E. coli*, suggesting that the antibacterial effects of C91 result from the inhibition of *Hp*IMPDH rather than an off-target effect.

Implications for the Design of Antibiotics Targeting IMPDH

The above findings indicate that Ala165 and Tyr358 comprise a structural motif that defines enzymes susceptible to *Cp*IMPDH inhibitors. A BLAST search reveals that these critical residues are present in IMPDHs from a wide variety of pathogenic bacteria in addition to *C. parvum*, *B. burgdorferi*, *H. pylori* and *S. pyogenes.* Importantly, this list includes select agents and multidrug resistant bacteria, where new antibiotics are urgently needed, but not *E. coli* (Table S1). As shown in Figure 2E, the inhibitor binding site is highly conserved among *C. parvum* and pathogenic bacteria, suggesting that IMPDH inhibition provides a promising strategy for the development of a broader spectrum antibiotic. Prokaryotic-specific inhibitors such as **C91** will be invaluable in validating IMPDH as a target for antibiotic chemotherapy that will spare commensal bacteria.

SIGNIFICANCE

The rising tide of antibiotic resistance creates an urgent need for new drugs to treat bacterial infections, but years of neglect have depleted the antibiotic pipeline. The repurposing of other drug development programs for antibiotic discovery is a promising strategy to address this problem. Inosine 5′-monophosphate dehydrogenase (IMPDH), a key enzyme in the biosynthesis of the precursors for RNA and DNA, presents an intriguing opportunity for such repurposing. IMPDH is a promising target for drugs against the protozoan parasite *Cryptosporidium parvum*, a major cause of diarrhea and malnutrition and a potential bioterrorism agent. Curiously, *Cp*IMPDH is most closely related to prokaryotic IMPDHs, suggesting that the parasite obtained its *IMPDH* gene via horizontal transfer. We previously identified inhibitors of *Cp*IMPDH that do not inhibit human IMPDHs. Here we show that selective inhibitors of *Cp*IMPDH also inhibit IMPDHs from the pathogenic bacteria *Helicobacter pylori*, *Borrelia burgdorferi*, and *Streptococcus pyogenes*, but not *Escherchia coli*. Importantly, a second-generation *Cp*IMPDH inhibitor blocks *H. pylori* growth, demonstrating that these compounds have antibacterial activity. Susceptible enzymes are defined by a structural motif that is found in IMPDHs from a wide variety of pathogenic bacteria, suggesting that IMPDH-targeted inhibitors can be developed into a new class of broader spectrum antibiotics that will spare some commensal bacteria.

EXPERIMENTAL PROCEDURES

Materials

Compounds **D**, **E**, **F**, **G**, and **H** were purchased from ChemDiv Inc. (San Diego, CA), Compounds **A**, **B**, and **C** were synthesized as described previously (Umejiego et al., 2008). Compound **C91** was synthesized as described in Supplemental Experimental Procedures. All other chemicals were obtained from Fisher Scientific, unless mentioned otherwise. Plasmid containing the *guaB* gene of *S. pyogenes* was a generous gift of Dr. Cameron Ashbaugh (Ashbaugh and Wessels, 1995). *H. pylori* total genomic DNA was obtained from American Type Culture Collection (ATCC). *L. donovani* IMPDH coding sequence was the gift of Dr. Buddy Ullman (Wilson et al., 1991).

Enzyme Cloning and Purification

Recombinant *T. foetus*, *B. burgdorferi, E. coli* and *C. parvum* IMPDH were expressed in Δ*guaB* strains of *E. coli* (which lack endogenous IMPDH) and purified as described previously (Digits and Hedstrom, 1999; Kerr and Hedstrom, 1997; Umejiego et al., 2004; Zhou et al., 1997). The S250A, L444Y, and S250A/L444Y mutants of *E. coli* IMPDH were constructed using Quikchange (Stratagene, La Jolla, CA). Enzymes were expressed and purified as previously described (Kerr and Hedstrom, 1997).

To express *L. donovani* IMPDH, a NcoI site was created at the beginning of the *Ld*IMPDH coding sequence and the NcoI-PstI fragment was cloned into pKK233-2 to create the plasmid pLDI, which expresses *Ld*IMPDH under control of the *trc* promoter. Cultures were induced with 0.5 mM IPTG and grown overnight. Cells were harvested by centrifugation, resuspended in 50 mM Tris-HCl (pH 8.0), 1 mM dithiothreitol, and 10% glycerol (Buffer A), lysed by sonication and clarified by centrifugation followed by filtration through a 45 μm cellulose acetate filter. Protein was applied to a Poros HS strong cation exchange resin (PerSeptive Biosystems) pre-equilibrated with 20 mM sodium phosphate buffer (pH 7.5), 1 mM dithiothreitol (Buffer B). *Ld*IMPDH was eluted with a gradient of 0–0.9 M NaCl. Fractions containing IMPDH activity were pooled and applied to IMP affinity resin. The column was washed with Buffer B and enzyme was eluted with Buffer B containing 0.5 M KCl, 1 mM IMP. The specific activity of the final preparation was 2.6 μmol/min-mg.

The *H. pylori* and *S. pyogenes guaB* genes were cloned into pET28a with 6x His-tags. Bacteria were grown at 30°C in LB medium containing 25 μg/ml

kanamycin until the OD_{600} reached approximately 0.6. Expression was initiated by the addition of 0.5 mM IPTG and the temperature was changed to 25°C. Bacteria were harvested after 16 hr. The cell pellet was rinsed (3x) with 50 mM phosphate buffer, 500 mM NaCl, 5 mM imidazole (pH 8.0), 1 mM IMP, and 5 mM β-mercaptoethanol, and lysed by sonication. The lysate was clarified by centrifugation and loaded on a Ni-NTA column (QIAGEN). The purified protein were eluted in 50 mM phosphate buffer, 500 mM NaCl, 250 mM imidazole (pH 8.0), 1 mM IMP, and 5 mM β-mercaptoethanol, concentrated, and dialyzed against Buffer A. The protein concentration was determined by using Bradford dye procedure (Bio-Rad).

Steady-State Enzyme Kinetics

IMPDH assays were performed in 50 mM Tris-HCl (pH 8.0), 100 mM KCl, 3 mM EDTA, and 1 mM DTT. Activity was routinely assayed in the presence of 50 nM IMPDH at 25°C. NADH production was monitored either by following absorbance change at 340 nm using a Hitachi U-2000 spectrophotometer (ε = 6.2 mM^{-1} cm^{-1}). IMPDHs are prone to NAD^+ substrate inhibition (Hedstrom, 2009). Therefore, the steady-state kinetics for *Hp*IMPDH were initially analyzed by varying NAD^+ at saturating IMP concentrations to determine the value of K_m for NAD^+, then by varying IMP at the fixed NAD^+ concentration as close to saturating as practical. Using the SigmaPlot program (SPSS, Inc.), initial velocity data were fit to the Michaelis-Menten equation (Equation 1) and/or the uncompetitive substrate inhibition equation (Equation 2), as follows:

$$v = V_m[S]/(K_m + [S]) \quad (1)$$

$$v = V_m/\left(1 + K_m/[S] + [S]^2/K_{ii}\right), \quad (2)$$

where v represents the velocity, V_m is the maximal velocity, S is the substrate concentration, K_m is the Michaelis constant, K_{ii} is the intercept inhibition constant. The values of k_{cat} determined under both conditions are in good agreement.

Inhibitor Kinetics

Enzyme was incubated with inhibitor (50 pM to 100 μM) for 10 min at room temperature prior to addition of substrates. The conditions used for each enzyme is listed in Supplemental Experimental Procedures. IC_{50} values were calculated for each inhibitor according to Equation 3 using the SigmaPlot program (SPSS, Inc.):

$$\upsilon_i = \upsilon_0/(1 + [I]/IC_{50}), \quad (3)$$

where υ_i is initial velocity in the presence of inhibitor (I) and υ_0 is the initial velocity in the absence of inhibitor.

Assays were carried out in assay buffer at 25°C with ~50 nM IMPDH and NADH production was monitored by following fluorescence. The values of K_i with respect to NAD^+ were determined by using fixed concentrations of IMP and varied NAD^+ concentrations. Data were fitted according to Equation 4 (noncompetitive inhibition) using SigmaPlot program (SPSS, Inc.):

$$\upsilon = V_m[S]/\{K_m(1 + [I]/K_{is}) + [S](1 + [I]/K_{ii})\}, \quad (4)$$

where K_{ii} and K_{is} represent the intercept and slope inhibition constants, respectively. The best fits were determined by the relative fit error. The Morrison equation was used to evaluate tight-binding inhibitors (Morrison, 1969).

Determination of K_c

The values of K_c were determined by measuring the interaction between tiazofurin and ADP (Digits and Hedstrom, 2000; Hedstrom and Wang, 1990). Tiazofurin binds in the nicotinamide subsite of the NAD site while ADP binds in the adenosine subsite. If the closed conformation is favored, tiazofurin and ADP will interact synergistically; one inhibitor shifts the enzyme into the open conformation and promotes the association of the second inhibitor (Guillén Schlippe et al., 2004). If the open conformation is favored, the two inhibitors bind independently. Tiazofurin and ADP concentrations are varied at constant IMP and NAD^+. Initial velocities were fit to Equation 5 using SigmaPlot:

$$v = v_0/[1 + [I]/K_i + [J]/K_j + [I][J]/\alpha K_i K_j], \quad (5)$$

where v is the initial velocity, v_0 is the initial velocity in the absence of inhibitor, K_i and K_j are the inhibition constants for the inhibitors I and J, respectively, and α is the interaction constant. The value of α approximates the fraction of enzyme in the open conformation, so the value of K_c is obtained (Guillén Schlippe et al., 2004):

$$K_c = (1 - \alpha)/\alpha. \quad (6)$$

Bacterial Growth Assays

H. pylori strain G27 (Baltrus et al., 2009) was stored at −80°C in Brucella broth (Becton Dickinson) supplemented with 10% fetal bovine serum (FBS) and 20% glycerol. Bacteria were plated on TSA/sheep blood agar plates (Remel) or grown in growth media (Brucella broth supplemented with 10% FBS and 4 μg/ml fungizone/amphotericin B) at 37°C in a 10% CO_2 incubator. For growth inhibition assays, a frozen stock of *H. pylori* strain G27 was plated on blood agar plates and allowed to grow for 48 hr. The bacteria were resuspended in growth media (30 ml) and incubated for ~18–20 hr. The resulting stationary phase bacteria were diluted into assay media (Brucella broth with 10% FBS) to an OD_{600} = 0.025 (~10^4 colony forming units/μl) and aliquots (200 μl) were added to 96-well tissue-culture grade polystyrene plates (Costar, Corning Inc.). A DMSO solution of **C91** (2 μl) was added to each well and the plates were incubated with shaking. Colony forming units (CFUs) were measured by diluting aliquots at 0, 2, 4, 8, 12, and 24 hr, and plating on blood agar plates. Alternatively, logarithmic phase bacteria were obtained by diluting stationary phase bacteria 5x into fresh growth media (25 ml) and incubating with shaking for 4 hr prior to the growth inhibition assay.

An exponentially growing culture of *E. coli* MG1655 was diluted into fresh Luria broth containing C91 (100 and 200 μM) or DMSO. The triplicate cultures were incubated at 37°C in a plate reader and optical density was recorded every minute over 3.5 hr.

SUPPLEMENTAL INFORMATION

Supplemental Information includes Supplemental Experimental Procedures and four figures and two tables and can be found with this article online at doi:10.1016/j.chembiol.2010.07.014.

ACKNOWLEDGMENTS

This work was supported by NIH-NIAID U01 AI075466 (L.H.). GWL was supported in part by the University of Virginia Cancer Training Grant (5T32 CA 009109).

Received: March 28, 2010
Revised: June 26, 2010
Accepted: July 20, 2010
Published: October 28, 2010

REFERENCES

Abrahamsen, M.S., Templeton, T.J., Enomoto, S., Abrahante, J.E., Zhu, G., Lancto, C.A., Deng, M., Liu, C., Widmer, G., Tzipori, S., et al. (2004). Complete genome sequence of the apicomplexan, *Cryptosporidium parvum*. Science *304*, 441–445.

Ashbaugh, C.D., and Wessels, M.R. (1995). Cloning, sequence analysis and expression of the group A streptococcal *guaB* gene encoding inosine monophosphate dehydrogenase. Gene *165*, 57–60.

Baltrus, D.A., Amieva, M.R., Covacci, A., Lowe, T.M., Merrell, D.S., Ottemann, K.M., Stein, M., Salama, N.R., and Guillemin, K. (2009). The complete genome sequence of *Helicobacter pylori* strain G27. J. Bacteriol. *191*, 447–448.

Bapteste, E., and Philippe, H. (2002). The potential value of indels as phylogenetic markers: position of trichomonads as a case study. Mol. Biol. Evol. *19*, 972–977.

Colby, T.D., Vanderveen, K., Strickler, M.D., Markham, G.D., and Goldstein, B.M. (1999). Crystal structure of human type II inosine monophosphate dehydrogenase: implications for ligand binding and drug design. Proc. Natl. Acad. Sci. USA *96*, 3531–3536.

Digits, J.A., and Hedstrom, L. (1999). Kinetic mechanism of *Tritrichomonas foetus* inosine-5′-monophosphate dehydrogenase. Biochemistry *38*, 2295–2306.

Digits, J.A., and Hedstrom, L. (2000). Drug selectivity is determined by coupling across the NAD^+ site of IMP dehydrogenase. Biochemistry *39*, 1771–1777.

Dobie, F., Berg, A., Boitz, J.M., and Jardim, A. (2007). Kinetic characterization of inosine monophosphate dehydrogenase of *Leishmania donovani*. Mol. Biochem. Parasitol. *152*, 11–21.

Fayer, R. (2004). *Cryptosporidium*: a water-borne zoonotic parasite. *Veterinary Parasitology*. Vet. Parasitol. *126*, 37–56.

Fischbach, M.A., and Walsh, C.T. (2009). Antibiotics for emerging pathogens. Science *325*, 1089–1093.

Gan, L., Petsko, G.A., and Hedstrom, L. (2002). Crystal structure of a ternary complex of *Tritrichomonas foetus* inosine 5′-monophosphate dehydrogenase: NAD+ orients the active site loop for catalysis. Biochemistry *41*, 13309–13317.

Gan, L., Seyedsayamdost, M.R., Shuto, S., Matsuda, A., Petsko, G.A., and Hedstrom, L. (2003). The immunosuppressive agent mizoribine monophosphate forms a transition state analog complex with IMP dehydrogenase. Biochemistry *42*, 857–863.

Guillén Schlippe, Y.V., and Hedstrom, L. (2005a). Guanidine derivatives rescue the Arg418Ala mutation of *Tritrichomonas foetus* IMP dehydrogenase. Biochemistry *44*, 16695–16700.

Guillén Schlippe, Y.V., and Hedstrom, L. (2005b). Is Arg418 the catalytic base required for the hydrolysis step of the IMP dehydrogenase reaction? Biochemistry *44*, 11700–11707.

Guillén Schlippe, Y.V., Riera, T.V., Seyedsayamdost, M.R., and Hedstrom, L. (2004). Substitution of the conserved Arg-Tyr dyad selectively disrupts the hydrolysis phase of the IMP dehydrogenase reaction. Biochemistry *43*, 4511–4521.

Hedstrom, L. (2009). IMP dehydrogenase: structure, mechanism and inhibition. Chem. Rev. *109*, 2903–2928.

Hedstrom, L., and Wang, C.C. (1990). Mycophenolic acid and thiazole adenine dinucleotide inhibition of *Tritrichomonas foetus* inosine 5′-monophosphate dehydrogenase: implications on enzyme mechanism. Biochemistry *29*, 849–854.

Kerr, K.M., and Hedstrom, L. (1997). The roles of conserved carboxylate residues in IMP dehydrogenase and identification of a transition state analog. Biochemistry *36*, 13365–13373.

Kohler, G.A., Gong, X., Bentink, S., Theiss, S., Pagani, G.M., Agabian, N., and Hedstrom, L. (2005). The functional basis of mycophenolic acid resistance in *Candida albicans* IMP dehydrogenase. J. Biol. Chem. *280*, 11295–11302.

MacPherson, I.S., Kirubakaran, S., Gorla, S.K., Riera, T.V., D'Aquino, J.A., Zhang, M., Lu, J., Cuny, G.D., and Hedstrom, L. (2010). The structural basis of *cryptosporidium*-specific IMP dehydrogenase inhibitor selectivity. J. Am. Chem. Soc. *132*, 1230–1231.

Maurya, S.K., Gollapalli, D.R., Kirubakaran, S., Zhang, M., Johnson, C.R., Benjamin, N.N., Hedstrom, L., and Cuny, G.D. (2009). Triazole inhibitors of *Cryptosporidium parvum* inosine 5′-monophosphate dehydrogenase. J. Med. Chem. *52*, 4623–4630.

McMillan, F.M., Cahoon, M., White, A., Hedstrom, L., Petsko, G.A., and Ringe, D. (2000). Crystal structure at 2.4 Å resolution of *Borrelia burgdorferi* inosine 5′-monophosphate dehydrogenase: evidence of a substrate-induced hinged-lid motion by loop 6. Biochemistry *39*, 4533–4542.

Miller, J.R., Dunham, S., Mochalkin, I., Banotai, C., Bowman, M., Buist, S., Dunkle, B., Hanna, D., Harwood, H.J., Huband, M.D., et al. (2009). A class of selective antibacterials derived from a protein kinase inhibitor pharmacophore. Proc. Natl. Acad. Sci. USA *106*, 1737–1742.

Min, D., Josephine, H.R., Li, H., Lakner, C., MacPherson, I.S., Naylor, G.J., Swofford, D., Hedstrom, L., and Yang, W. (2008). An enzymatic atavist revealed in dual pathways for water activation. PLoS Biol. *6*, e206. 10.1371/journal.pbio.0060206.

Morrison, J.F. (1969). Kinetics of reversible inhibition of enzyme catalyzed reactions by tight binding inhibitors. Biochim. Biophys. Acta *185*, 269–286.

Pettersen, E.F., Goddard, T.D., Huang, C.C., Couch, G.S., Greenblatt, D.M., Meng, E.C., and Ferrin, T.E. (2004). UCSF Chimera- a visualization system for exploratory research and analysis. J. Comput. Chem. *25*, 1605–1612.

Prosise, G.L., and Luecke, H. (2003). Crystal Structures of tritrichomonas foetus inosine monophosphate dehydrogenase in complex with substrate, cofactor and analogs: a structural basis for the random-in ordered-out kinetic mechanism. J. Mol. Biol. *326*, 517–527.

Prosise, G.L., Wu, J.Z., and Luecke, H. (2002). Crystal structure of tritrichomonas foetus inosine monophosphate dehydrogenase in complex with the inhibitor ribavirin monophosphate reveals a catalysis-dependent ion-binding site. J. Biol. Chem. *277*, 50654–50659.

Riera, T.V., Wang, W., Josephine, H.R., and Hedstrom, L. (2008). A kinetic alignment of orthologous inosine-5′-monophosphate dehydrogenases. Biochemistry *47*, 8689–8696.

Selgrad, M., and Malfertheiner, P. (2008). New strategies for *Helicobacter pylori* eradication. Curr. Opin. Pharmacol. *8*, 593–597.

Sintchak, M.D., Fleming, M.A., Futer, O., Raybuck, S.A., Chambers, S.P., Caron, P.R., Murcko, M., and Wilson, K.P. (1996). Structure and mechanism of inosine monophosphate dehydrogenase in complex with the immunosuppressant mycophenolic acid. Cell *85*, 921–930.

Sintchak, M.D., and Nimmesgern, E. (2000). The structure of inosine 5′-monophosphate dehydrogenase and the design of novel inhibitors. Immunopharmacology *47*, 163–184.

Striepen, B., Pruijssers, A.J., Huang, J., Li, C., Gubbels, M.J., Umejiego, N.N., Hedstrom, L., and Kissinger, J.C. (2004). Gene transfer in the evolution of parasite nucleotide biosynthesis. Proc. Natl. Acad. Sci. USA *101*, 3154–3159.

Striepen, B., White, M.W., Li, C., Guerini, M.N., Malik, S.B., Logsdon, J.M., Jr., Liu, C., and Abrahamsen, M.S. (2002). Genetic complementation in apicomplexan parasites. Proc. Natl. Acad. Sci. USA *99*, 6304–6309.

Tomb, J.F., White, O., Kerlavage, A.R., Clayton, R.A., Sutton, G.G., Fleischmann, R.D., Ketchum, K.A., Klenk, H.P., Gill, S., Dougherty, B.A., et al. (1997). The complete genome sequence of the gastric pathogen *Helicobacter pylori*. Nature *388*, 539–547.

Umejiego, N.N., Li, C., Riera, T., Hedstrom, L., and Striepen, B. (2004). *Cryptosporidium parvum* IMP dehydrogenase: identification of functional, structural and dynamic properties that can be exploited for drug design. J. Biol. Chem. *279*, 40320–40327.

Umejiego, N.N., Gollapalli, D., Sharling, L., Volftsun, A., Lu, J., Benjamin, N.N., Stroupe, A.H., Riera, T.V., Striepen, B., and Hedstrom, L. (2008). Targeting a prokaryotic protein in a eukaryotic pathogen: identification of lead compounds against cryptosporidiosis. Chem. Biol. *15*, 70–77.

Walsh, C.T., and Fischbach, M.A. (2009). Repurposing libraries of eukaryotic protein kinase inhibitors for antibiotic discovery. Proc. Natl. Acad. Sci. USA *106*, 1689–1690.

Whitby, F.G., Luecke, H., Kuhn, P., Somoza, J.R., Huete-Perez, J.A., Philips, J.D., Hill, C.P., Fletterick, R.J., and Wang, C.C. (1997). Crystal structure of *Tritrichomonas foetus* inosine-5′-monophosphate dehydrogenase and the enzyme-product complex. Biochemistry *36*, 10666–10674.

Wilson, K., Collart, F., Huberman, E., Stringer, J., and Ullman, B. (1991). Amplification and molecular cloning of the IMP dehydrogenase gene of *Leishmania donovani*. J. Biol. Chem. *266*, 1665–1671.

Zhang, R., Evans, G., Rotella, F., Westbrook, E., Huberman, E., Joachimiak, A., and Collart, F.R. (1999a). Differential signatures of bacterial and mammalian IMP dehydrogenase enzymes. Curr. Med. Chem. *6*, 537–543.

Zhang, R., Evans, G., Rotella, F.J., Westbrook, E.M., Beno, D., Huberman, E., Joachimiak, A., and Collart, F.R. (1999b). Characteristics and crystal structure of bacterial inosine-5′-monophosphate dehydrogenase. Biochemistry *38*, 4691–4700.

Zhou, X., Cahoon, M., Rosa, P., and Hedstrom, L. (1997). Expression, purification and charcterization of inosine-5′-monophosphate dehydrogenase from *Borrelia burgdorferi*. J. Biol. Chem. *272*, 21977–21981.